OTC 25511

Targeted Full-Waveform Inversion of Ground-Penetrating Radar Data for Quantification of Oil Spills under Sea Ice

John H. Bradford, and HP Marshall, Boise State University, Esther Babcock, Schlumberger Oilfield Services, David F. Dickins, DF Dickins Associates LLC.

Summary

We have implemented a targeted ground-penetrating radar (GPR) full-waveform inversion algorithm to quantify the physical characteristics of oil spills under and within sea-ice. We can invert for oil thickness, electric permittivity, and conductivity or any subset of these parameters if the others are known. We tested the algorithm with data collected during a controlled spill experiment at the US Army's Cold Regions Research and Engineering Lab (CRREL). Using 500 MHz radar reflection data, the algorithm recovered the thickness of a 5 cm thick oil layer to within 8% of the control value. This approach provides a tool for rapid spill detection and mapping that is needed with increasing levels of oil exploration and production in the Arctic environment.

Introduction

Increased interest in oil and gas development in Arctic regions is driving the need to develop rapid and effective methods for oil spill characterization and remediation in the sea-ice environment. For example, crude oil released from a subsea blowout, or a marine pipeline rupture, will rise through the water column to the surface. If an ice sheet is present, the oil will become trapped at the base of the ice forming an oil layer between the ice and water. Ocean currents and natural variations under the ice provide natural "reservoirs" to effectively contain spilled oil and can determine the areal distribution of oil. Spills under ice during the active solid ice growth period (typically October to April in many Arctic areas) will become encapsulated by new ice growth beneath the oil layer.

GPR has been shown to be effective for qualitative location of oil spills within sea-ice and trapped at the ice/water interface (e.g. Bradford et al., 2008; Bradford et al. 2010). Critical for effective clean up response, however, is not only spill location but also a quantitative assessment of the oil distribution. We have implemented a targeted GPR full-waveform inversion algorithm for quantifying oil spill electrical properties and thickness in the sea ice environment. Below, we describe the algorithm and the results of its application to a controlled spill test conducted at CRREL.

Method

The forward model consists of two components, 1) a sea ice electrical property model based on measurements of ice temperature and salinity, and 2) a 1D wave propagator implemented using the reflectivity method. The inversion algorithm operates in the time domain and minimizes the difference between the measured and modeled data

Electric property model

The properties that control electromagnetic wave propagation include the electric permittivity and electric conductivity. Sea ice is a complex mixture of brine and ice crystals. In natural sea ice the crystals are often aligned with the predominant current leading to azimuthal anisotropy in the ice electrical properties. Further, the electrical properties depend on temperature and salinity. Because of this complexity, it is necessary to use a set of empirical relationships to derive the electrical properties. For this study an electric property algorithm was employed based on the relationships given by Morey et al (1984). The algorithm proceeds as follows:

1. Input the measured temperature (T) and bulk salinity profile (S)
2. Compute brine volume (V_b) as a function of T and S
3. Compute the brine salinity (S_b) as a function of T
4. Compute the brine conductivity (σ_b) as a function of S_b and T
5. Compute the complex electric permittivity of the brine ε_b
6. Compute the bulk electric conductivity using Archie's law as a function of V_b and σ_b and imaginary component of ε_b, then output to wave propagator. Simulation of the electric field polarized either parallel or perpendicular to the ice crystal alignment is accomplished through choice of the Archie's law exponent.
7. Using an anisotropic mixing formula, compute the bulk real effective permittivity as a function of V_b , the real component of ε_b, and the permittivity of crystalline ice, then output to wave propagator.

The brine conductivity is given by an empirical relation as a function of temperature and salinity. The Archie's law exponent, m, is set to 1.5 for parallel polarization or 1.75 for perpendicular polarization relative to ice crystal alignment. Taylor's (1965) anisotropic mixing formula simulates the sea ice permittivity by using the permittivity of pure ice as the host material and the Debye relaxation model for brine as the inclusion.

Wave Propagator

The reflectivity method is an exact analytical solution to the electromagnetic wave equation for plane waves propagating through a 1D medium. The radar response is computed in a layered model using a recursion formula that correctly simulates primary and multiple reflections (Meuller, 1985). We carry out the computation in the frequency domain with frequency dependent material properties as described above. The properties of each layer are constant, but the model incorporates smoothly varying vertical changes in material properties by dividing the model into many thin layers with small changes between each layer. The thin layers must be well below the scattering limit (~1/10 – 1/30 of a wavelength) for the radar wavelet being modeled. The source wave for the code is a plane wave at normal incidence.

Inversion Algorithm

In the inversion algorithm, we take a targeted approach and minimize the difference between the model and field data for a target reflection or a targeted set of reflections. This approach minimizes the non-uniqueness and complexity of the inverse problem. We first estimate the ice electrical properties based on ice core measurements of temperature and salinity. For the starting model, we then insert a layer or layers of oil at the expected location within the ice or at the base of the ice. The inversion then optimizes for oil layer thickness, oil permittivity, and oil conductivity. We minimize the difference between the field and model data over the targeted region in a least squares sense using the multi-parameter Nelder-Mead simplex method. We may also optionally include finding the optimal effective source function and total ice thickness.

Data Example

The project utilized the Geophysical Research Facility at CRREL to develop a test sea ice sheet. This facility consists of a concrete basin, 18.25 m long x 6.7 m wide x 2 m deep, with a removable roof that maintains a growing ice cover in a refrigerated ambient environment and protects it from snow. Growth of the 80-90 cm thick ice sheet occured between December and February 2011.

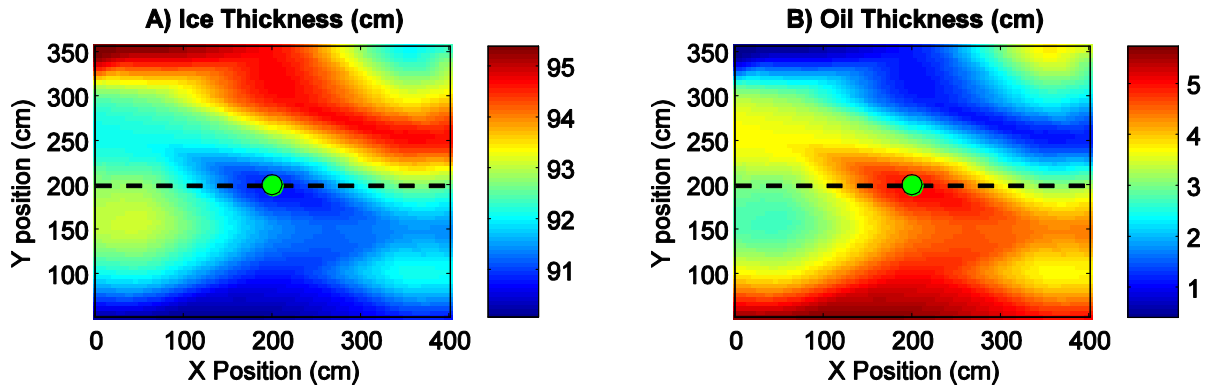

Figure 1. Contour of ice thickness made from 35 borehole measurements on a 20 x 60 cm grid. Oil thickness is computed from the total volume of oil spilled with the upper surface following under ice topography and the lower surface forming a horizontal horizon with the water surface. Note the correlation in oil thickness with GPR attributes shown in Figure 2. The oil is just over 5 cm thick at the location of the GPR trace used for inversion which is shown with the green dot.

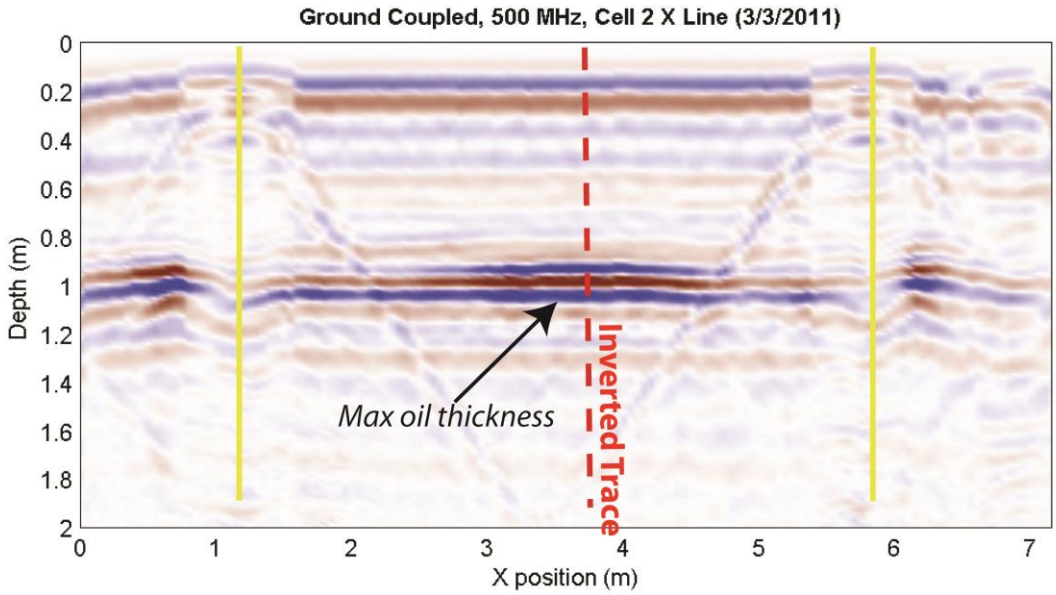

Figure 2. GPR profile crossing containment cell with oil spilled at the base of the ice. Yellow lines indicate Cell boundaries. The effect of oil is qualitatively evident as an increase in reflection amplitude toward the center of the cell where the oil reaches its maximum thickness of just over 5 cm.

CRREL staff conducted two crude oil spills, the first on February 18 prior to testing to allow the oil to become encapsulated by new ice growth, and the second on March 2 during GPR data acquisition. In each case a discharge hose was positioned in the center of a 4x4 m containment hoop via a trolley system along the basin bottom. The containment hoops consisted of plastic sheeting that was frozen in during ice growth. These hoops extended approximately 30 cm beneath the base of the ice to control the oil distribution. We measured the relative electric permittivity of the crude oil with a TDR probe and found it to be 3.1.

For each spill, approximately 0.57 m^3 of crude oil was discharged into each test hoop. This volume translates to an average film thickness of 3.6 cm, but the actual distribution is non-uniform due to ice irregularity. On March 4, following completion of the radar surveys, CRREL personnel documented the ice properties (temperature and salinity), ice thickness, and oil distribution through a series of cores and drillholes. Figure 1 shows measured ice thickness and estimated oil thickness for the second spill based on oil volume and under ice topography calculations. Note the irregular ice thickness distribution and the variable oil thickness ranging from about 0.5 cm to just under 6 cm. Even over this small 4x4 m area, the few cms of ice topography result in a highly irregular oil thickness distribution. Figure 2 shows a 500 MHz radar profile collected across the containment cell for the second spill. Note that there is an obvious increase in amplitude of the base of ice reflection that correlates with the increasing oil thickness near the center of the containment cell. A corresponding phase and frequency anomaly is also associated with the increase in oil thickness. These changes in waveform are caused by interference between reflections from the top and bottom of the thin layer of oil. At 500 MHz, the GPR wavelength in ice is about 20 cm near the base of the ice. The maximum oil thickness of 6 cm is just above the ¼ wavelength limit of the conventional resolution significant and measurable changes to the waveform occur well below this thickness.

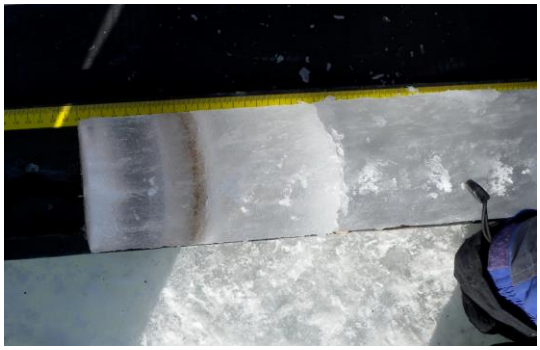

Figure 3. Photograph of an ice core taken from outside the containment cells showing a thin (<1 cm) sheen of oil droplets located ~ 9 cm above the base of the ice. This thin layer produced a measurable GPR response even at the relatively long wavelength of 25-30 cm of the 500 MHz signal.

Note also that a band of fine oil droplets approximately 1 cm thick was observed roughly 9 cm from the bottom of the cores throughout the tank (Figure 3). We believe that, due to shearing, a very small percentage of oil drifted laterally as fine droplets beyond the skirt boundaries during the first oil injection and was incorporated in the growing ice interface throughout the tank. This layer produced a measurable reflection in the GPR data. Thus we included the trapped layer in our property model and as a parameter in our inversion.

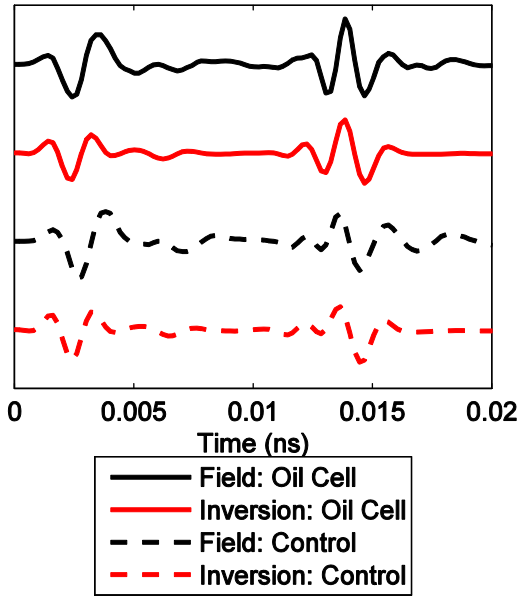

Figure 4. Comparison of field and inverted traces in the oiled and control (no oil) areas. We inverted for the effective source function using the control trace and then used this function in the inversion for oil thickness in the oiled cell.

For the example shown here, we first used a trace taken from an area outside the oil containment cells in an area of clean ice (Figure 4) and refer to this trace as the control trace. We inverted for the phase and amplitude of the effective source function using a 500 MHz Gabor wavelet. We also inverted for the thickness and position of the thin oil sheen located above the base of the ice. After performing this initial inversion, we inverted a trace from the center of the containment cell with oil at the base of the ice (Figure 4). For this inversion we used the effective source function from the first inversion and held it fixed. We used the ice property model and the oil sheen thickness and position as the starting model and then inverted for oil thickness at the base of the ice and the thickness and position of the thin oil sheen contained within the ice. In both cases we held the relative electric permittivity of the oil fixed at the measured value of 3.1.

Figure 4 shows a comparison of the field data traces with the model traces resulting from the inversion. The starting model parameters and inverted parameters are shown in Table 1. The inverted oil thickness differs by only 8% from that estimated by topography and volume calculations. Additionally, the inversion estimate of the thin oil sheen thickness is consistent with ice core measurements. The inverted oil sheen height above the base of the ice is 4 cm less than that outside of the test cell. This result is consistent with the observation that the ice thickness is less in the central part of the test cell where the inverted trace is taken – if the ice thickness were more uniform when the thin oil sheen was emplaced, then it should be closer to the base of ice in areas of thinner total ice thickness.

Table 1: Starting model parameters and inversion results. The sheen is the trapped thin layer of fine oil droplets, and h indicates its height above the base of the ice.

	Control trace		**Oil spill trace**		**Control**
	Start	***Final***	***Start***	***Final***	**data**
h_{sheen}	12.0 cm	10.0 cm	10.0 cm	5.6 cm	~9.0 cm
Δz_{sheen}	0.5 cm	1.3 cm	1.3 cm	1.4 cm	~1.0 cm
Δz_{oil}	--	--	3.5 cm	5.4 cm	5.0 cm

Conclusions

Targeted full-waveform inversion appears to be a promising approach to quantifying the thickness of oil spills that are trapped within ice and at the ice/water interface. The additional parameters of ice temperature and salinity along with oil electric permittivity improve the inversion result. These parameters could be obtained relatively quickly in a real spill scenario or estimated from historical data during the early stages of a response. The simple 1D inversion approach worked well in the controlled experiment conducted for this study. Sea ice growing in the ocean can be significantly more complicated with areas of rough, broken ice, variable snow cover, and a more irregular distribution of brine. For more general application, future work will need to be directed toward 2D and 3D heterogeneity and will perhaps require 2D and 3D inversions that include ice anisotropy.

Acknowledgements

We thank Len Zabilansky and the crew at CRREL's ice engineering lab for growing the ice, conducting the oil spills and supporting logistics for the project. The US Bureau of Ocean Management: Regulation and Enforcement (now BSEE), Alaska Clean Seas, Shell, Conoco Phillips, and Statoil funded this project.

References

Bradford, J. H., D. F. Dickins, and L. Liberty. 2008, Locating oil spills under sea ice using ground-penetrating radar. The Leading Edge, **27**, 1424-1435.

Bradford, J. H., D. F. Dickins, and P. J. Brandvik. 2010, Assessing the potential to detec oil spills in and under snow using airborne ground-penetrating radar. Geophysics, **75**, G1-G11. doi: 10.1190/1.3312184.

Morey, R. M., A. Kovacs, and G. F. N. Cox. 1984, Electromagnetic properties of sea ice. Cold Regions Science and Technology, **9**, 53-75.

Mueller, G. 1985, The reflectivity method: A tutorial. Journal of Geophysics, **58**, 153-174.

Taylor, L. 1965, Dielectric properties of mixtures. IEEE Transactions on Antennas and Propagation, **13**, 943-947.